Fuel 374 (2024) 132319

Contents lists available at ScienceDirect

Fuel

journal homepage: www.elsevier.com/locate/fuel

Full Length Article

Predictive modelling for coal abrasive index: Unveiling influential factors through Shallow and Deep Neural Networks

Moshood Onifade [a,*], Abiodun Ismail Lawal [b], Samson Oluwaseyi Bada [c,*], Manoj Khandelwal [a,*]

[a] Institute of Innovation, Science and Sustainability, Federation University Australia, Ballarat, VIC 3350, Australia
[b] Department of Mining Engineering, Federal University of Technology, Akure, Nigeria
[c] School of Chemical and Metallurgy, Faculty of Engineering and the Built Environment, University of the Witwatersrand, Johannesburg, South Africa

ARTICLE INFO

Keywords:
Abrasive index
Artificial intelligence
Coal
Hardgrove grindability index
South African coalfields

ABSTRACT

The use of coal in applications such as power generation is influenced by its combustibility, sulphur content, Hardgrove grindability index (HGI), and abrasivity index (AI), including its volatile matter and ash content, etc. Collectively, these properties affect the quality and performance of coal for its intended use. In particular, the abrasive characteristics of coal from both the same and different coal fields pose challenges during milling operations, leading to accelerated wear and tear of machinery within the plant. In this study, the abrasive index (AI) of coal samples from three South African coalfields using the Yancey, Geer, and Price (YGP) method was conducted. A predictive model using artificial intelligence was developed using the AI obtained from individual samples and other characteristics of the coals. A reliable model utilizing Shallow Neural Network (SNN) and Deep Neural Network (DNN) was developed to relate the coal properties to AI across the different coalfields tested. It is noteworthy that the DNN demonstrated superior performance in modeling AI for all three coalfields, with ash content being the most influential factor. The research findings underscore the importance of other coal properties, including volatile matter, fixed carbon, calorific value, and HGI, in forecasting coal AI. Furthermore, it contributed to the knowledge of the use of artificial intelligence, specifically for a diverse range of coal samples collected from various South African coalfields.

1. Introduction

Coal is a naturally occurring fossil fuel with a wide range of properties. Coal's burning characteristics reflect its organic component, which is more evident than its physicochemical properties [33]. The diverse properties of coal make it suitable for a variety of processes, such as gasification, and combustion, and as a reductant for metallurgical applications. The main components of coal are organic and inorganic matter [18,19,29]. Inorganic matter, also known as mineral matter, has a negative influence on various aspects of coal's combustion processes. It resulted in coal's unwelcome abrasion, slagging, fouling, corrosion, and erosive behavior [26,35,36]. The maceral, also known as the organic matter, is the component that is responsible for coal's high combustion efficiency. Volatile matter, fixed carbon, ash fusion temperatures, Hardgrove grindability index (HGI), abrasive index (AI), and calorific value are among the properties used to classify coal [3]. Some of these properties negatively influence the output of the boiler leading to agglomeration which could initiate slag on the walls of the boiler and superheaters [39]. Coals that lead to this effect have of high propensity to fouling, slagging, erosion, and corrosion, which mainly result from the coal's mineral content or ash composition Xie et al. [38].

The abrasiveness index (AI) of the coal, especially for pulverized fuel (PF) boilers, should be taken into account when deciding on the appropriate equipment for pulverizing coal [1]. The AI indicates the hardness of the coal and its impact on the surface wear and tear with which it interacts. Since wear and grinding of the equipment occur simultaneously, both factors will influence the total energy used by the plant to pulverize the coals, in particular the grinding nature of the coals. In other words, high power consumption is directly related to hard grinding materials, which in turn results in high wear on the mill steel component [24]. These minerals or materials are interlocked within the coal matrix or included in the run of mine (ROM) when the roof and floor of a seam are mined with the coal seam. The presence of minerals, such as quartz leads to significant wear in mills, resulting in the more

* Corresponding authors.
E-mail addresses: m.onifade@federation.edu.au (M. Onifade), Samson.Bada@wits.ac.za (S.O. Bada), m.khandelwal@federation.edu.au, mkhandelwal1@gmail.com (M. Khandelwal).

https://doi.org/10.1016/j.fuel.2024.132319
Received 11 February 2024; Received in revised form 7 April 2024; Accepted 22 June 2024
Available online 8 July 2024
0016-2361/© 2024 The Author(s). Published by Elsevier Ltd. This is an open access article under the CC BY license (http://creativecommons.org/licenses/by/4.0/).

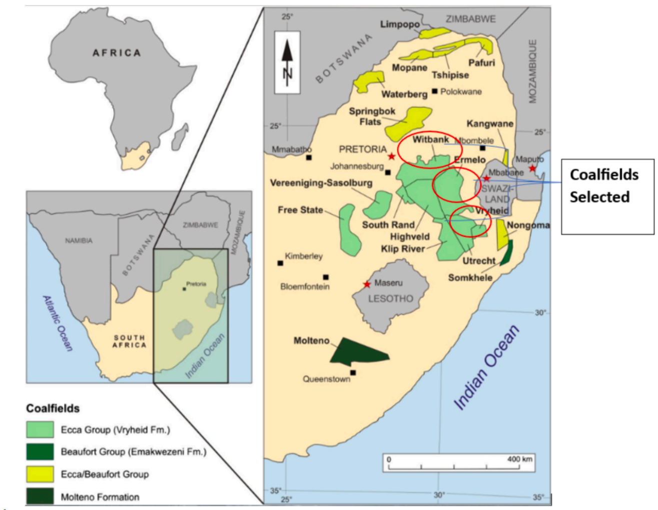

Fig. 1. Coalfields of South Africa. The Mopane, Tshipise and Pafuri Coalfields collectively form the Soutpansberg Coalfield. Fm. = Formation[30].

frequent replacement of mill liners and associated ducts [10]. In addition, this resulted in the regular replacement of boiler tubes and a reduction in the service life of other associated equipment. Most of the power plant's operating expenses are aimed at replacing worn-out components, which leads to downtime and power loss [15]. The cost of material replacement and maintenance for mills can be minimized by coal users by assessing the relative abrasion characteristics of their feed coal, taking into account the degradation of coal quality.

The coal's HGI is another distinct measurement index that is also closely related to AI [28]. It provides information on the ease of grinding coal and the power required for grinding coal in a pulverizer or mill. The energy or power utilized to grind coals can be influenced by wear and grinding, which are inseparable. In addition, hard grinding media also has a direct link with high power consumption. To determine the coal's AI index, the standard method used is BS 1016: Part 19: 1980, based on that established by Yancey, Geer, and Price [41]. The grindability of the coal was determined using the HGI method in accordance with [8]. Both methods have been identified as being laborious, time-consuming, and expensive [12]. For this reason and the importance of these characteristics in many coal applications, predictive models have always been necessary. In the case of the AI method, Yancey, Geer, and Price (YGP) appears to be the most commonly used method for determining the abrasive characteristics of coal. It has become standard in the United Kingdom, Australia, South Africa, and India, with Russia referring to it as the [27]. The repeatability of the data obtained by this method is predicted to be 10 % if the AI concentration is greater than 20 mg/kg and ± 2 mg/kg if it is lower. The approach has low repeatability and reproducibility, according to Tshiongo and Mulaba-Bafubiandi [34]. Furthermore, there are no comparative studies or estimates of the repeatability of measurements made at various laboratories included in the domestic standards for the method.

Many studies have been conducted by using machine learning to solve engineering problems [9,25,13,2] however, limited studies have been carried out by using machine learning to predict the AI of coals [37,10,17,14]. Some of the models are based on the inherent properties of coal, as the AI of coal is known to be controlled by its chemical, physical, and mechanical properties [31,32]. None of these studies have developed predictive models for AI of coals from various coalfields using artificial intelligence. This study is being conducted due to the fact that the abrasivity of coals is expected to vary based on the unique qualities of a deposit. As coal blending is a norm in the industry, developing a model based on a wide range of qualities from different fields is of importance to the industry. To achieve a better algorithm for achieving the set objectives, many experimental data were subdivided into groups based on certain characteristics.

In this study, an effort has been made to correlate the abrasive properties of coals from three South African coalfields to several properties such as moisture, volatile matter, ash content, fixed carbon, total sulphur, calorific value, pyrite content and HGI. For determining the AI value, each coal was divided into a variety of relative density fractions. The Shallow Neural Network (SNN) and Deep Neural Network (DNN) were used to develop predictive models and the relationships between the abrasive-related properties were established.

2. Sample collection, preparation, and testing

For this study, a total of 292 coal samples were obtained from three South African coalfields as shown in Fig. 1. 147 coal samples were taken from the Witbank coalfield, which encompasses Middleburg and Secunda. 56 coal samples from various mines were analysed from the Ermelo coalfield in Belfast, Carolina. In addition, 89 samples were collected from the KwaZulu Natal coalfields in Vryheid, Utrecht and Ulundi. These samples originate from different coalfields that were all formed in the Gondwana Karoo Basin between the Permian and mid-Triassic periods. Compared to carboniferous coal from the northern hemisphere, these coals are less mature and of lower rank. Upon receipt, the coal samples were crushed, blended and divided using a rotary splitter to generate different sub-samples in accordance with the [4] at different size fractions.

The proximate analysis was conducted in accordance with the [5]. Approximately 1 g of coal sample was used for the analyses in determining the inherent moisture, ash content and volatile matter present in the coal with fixed carbon calculated by difference. The ultimate and total sulphur analyses of the coals were performed according to [6]:2015 and [16]. The calorific value as the measure of the heat content was determined in accordance with [7]. The HGI was conducted in accordance with the [8]. For this test, 1 kg of coal sample was subjected to standard grinding conditions to pass through a 4.75 mm sieve. The resulting sample was staged screened to obtain a maximum representative sample between 1.18 mm and + 600 µm size fraction. A representative 50 g of the sized coal sample was taken in a ball mill along with 8 iron balls with a diameter of 25.4 ± 0.003 mm and turned for 60

Table 1
Descriptive statistics of the experimental parameters for Witbank coalfield.

Parameters	Symbols	N total	Mean	Std	Sum	Skewness	Kurtosis	Min	Median	Max
Calorific value	CV	147	26.920	2.157	3957.3	−0.645	0.179	19.5	27.5	31.2
Moisture	M	147	3.371	1.178	495.5	0.850	0.346	1.9	3.1	7.6
Ash	A	147	14.721	4.380	2164	0.837	1.297	6.6	14	32.4
Volatile matter	VM	147	26.329	2.759	3870.3	0.283	−0.185	20.1	26	33.1
Fixed carbon	FC	147	55.576	3.575	8169.7	−0.361	0.379	42.1	55.2	61.9
Total sulphur	TS	147	0.696	0.399	102.29	2.115	6.806	0.21	0.59	2.87
	Pyrite	147	0.820	0.688	120.57	2.1707	6.256	0.06	0.65	4.28
Hardgrove grindability index	HGI	147	54.959	5.712	8079	0.874	1.394	43	54	76
Abrasive index	AI	147	122.680	83.931	18034	1.864	4.721	15	96	515

*N total: Total number of samples; Std: standard deviation; Min: Minimum; Max: Maximum.

Table 2
Correlation coefficient matrix of experimental parameters for Witbank coalfield.

	CV	M	A	VM	FC	TS	Pyrite	HGI	AI
CV	1								
M	−0.47746	1							
A	−0.9036	0.099434	1						
VM	0.632039	−0.20064	−0.62618	1					
FC	0.77773	−0.29864	−0.77448	0.061746	1				
TS	−0.32233	−0.23659	0.446729	−0.13967	−0.36127	1			
Pyrite	−0.30619	−0.24538	0.435992	−0.1903	−0.30612	0.976519	1		
HGI	−0.70561	0.43535	0.575321	−0.72539	−0.2904	0.136141	0.107469	1	
AI	−0.55462	0.095677	0.638757	−0.16307	−0.68861	0.337208	0.3685	0.127638	1

Table 3
Descriptive statistics of the experimental parameters for Ermelo coalfield.

Parameters	Symbols	N total	Mean	Std	Sum	Skewness	Kurtosis	Min	Median	Max
Calorific value	CV	56	25.837	2.099	1446.89	−0.709	0.016	20.4	26.3	29.3
Moisture	M	56	3.866	1.095	216.5	−0.407	−0.655	1.7	4.05	5.8
Ash	A	56	17.020	4.283	953.1	0.832	0.326	9.2	15.7	28.6
Volatile matter	VM	56	23.745	6.348	1329.7	−0.986	0.918	7.7	24.3	34.5
Fixed carbon	FC	56	55.370	6.055	3100.7	1.631	2.673	45.8	54.1	74.7
Total sulphur	TS	56	0.731	0.326	40.91	0.233	−0.443	0.15	0.75	1.54
	Pyrite	56	0.757	0.488	42.4	0.924	0.838	0.06	0.67	2.23
Hardgrove grindability index	HGI	56	57.304	8.745	3209	0.395	−0.322	40	57	78
Abrasive index	AI	56	131.536	57.573	7366	1.821	6.055	37	124.5	387

Table 4
Correlation coefficient matrix of experimental parameters for Ermelo coalfield.

	CV	M	A	VM	FC	TS	Pyrite	HGI	AI
CV	1								
M	−0.56059	1							
A	−0.81014	0.032982	1						
VM	0.131661	0.341904	−0.51933	1					
FC	0.536368	−0.56262	−0.16882	−0.74289	1				
TS	0.165365	−0.40963	0.064266	0.143766	−0.1221	1			
Pyrite	−0.19027	−0.06256	0.260646	0.157331	−0.33799	0.848755	1		
HGI	−0.42981	0.135911	0.5655	−0.49737	0.096872	−0.08889	0.099942	1	
AI	−0.2119	−0.38692	0.561445	−0.42387	0.117235	0.16568	0.125435	0.306494	1

Table 5
Descriptive statistics of the experimental parameters for KwaZulu Natal coalfield.

Parameters	Symbols	N total	Mean	Std	Sum	Skewness	Kurtosis	Min	Median	Max
Calorific value	CV	89	29.798	1.527	2652	−0.233	−0.345	26.2	29.9	33.2
Moisture	M	89	1.819	0.515	161.9	0.896	1.987	0.9	1.8	3.9
Ash	A	89	13.394	3.443	1192.1	0.793	1.496	5.9	13.1	23.8
Volatile matter	VM	89	12.580	6.510	1119.6	1.126	0.218	5.2	9.6	30.3
Fixed carbon	FC	89	72.196	7.875	6425.4	−0.799	−0.478	55.3	74.9	84.5
Total sulphur	TS	89	1.111	0.641	98.9	2.826	9.815	0.44	0.98	4.26
	Pyrite	89	0.955	1.049	84.99	3.579	14.295	0.11	0.71	6.47
Hardgrove grindability index	HGI	89	54.281	13.946	4831	0.517	−0.692	33	52	85
Abrasive index	AI	89	89.831	51.324	7995	0.901	0.594	23	81	260

Table 6
Correlation coefficient matrix of experimental parameters for KwaZulu Natal coalfield.

	CV	M	A	VM	F	TS	Pyrite	HGI	AI
CV	1								
M	−0.36601	1							
A	−0.92587	0.098545	1						
VM	−0.18915	−0.14165	0.182042	1					
F	0.585343	0.008617	−0.59427	−0.89638	1				
TS	−0.37497	−0.21358	0.530468	0.163561	−0.35505	1			
Pyrite	−0.44046	−0.20377	0.6032	0.201368	−0.41731	0.941808	1		
HGI	−0.0013	−0.4673	0.211468	0.622188	−0.57529	0.460654	0.516545	1	
AI	−0.6015	0.283384	0.53795	−0.10071	−0.17233	0.206349	0.266392	−0.19555	1

Table 7
Simulated SNN structures.

Networks	Training	Testing	Validation	Overall	Training	Testing	Validation	Overall
	Witbank coalfield				Ermelo coalfield			
8–2-1	0.86044	0.84371	0.87278	0.85995	0.78661	0.88664	0.82403	0.80108
8–3-1	0.92365	0.90797	0.894	0.91455	0.9742	0.84432	0.88959	0.96132
8–4-1	0.94127	0.9402	0.94604	0.94159	0.98011	0.98524	0.71202	0.97667
8–5-1	0.95446	0.9569	0.97898	0.96322	0.99358	0.67324	0.98738	0.98255
8–6-1	0.96869	0.98193	0.97053	0.97047	0.99205	0.99628	0.9981	0.99522
8–7-1	0.9759	0.97715	0.95647	0.97503	0.99852	0.9927	0.98875	0.99491
8–8-1	0.97883	0.96264	0.98406	0.97723	0.99182	0.99557	0.99001	0.99197
8–9-1	0.97946	0.98852	0.98513	0.98094	0.98771	0.97495	0.98882	0.98464
8–10-1	0.95969	0.91326	0.97046	0.95537	0.99914	0.99842	0.99022	0.99856
8–11-1	0.95357	0.96892	0.92005	0.95071	0.99853	0.99984	0.99956	0.99916
8–12-1	0.97856	0.95288	0.97682	0.97513	*0.99997*	*0.99999*	*0.99955*	*0.99995*
8–13-1	0.98265	0.935	0.97164	0.97997	0.99915	0.46344	0.99995	0.98874
8–14-1	0.95656	0.97334	0.9703	0.95917	0.99535	0.99962	0.99922	0.99783
8–15-1	0.95198	0.95228	0.98383	0.95669	0.99491	0.99121	0.99525	0.99473
8–16-1	0.98525	0.95519	0.98473	0.98252	0.99502	0.99589	0.97782	0.9932
8–17-1	0.9824	0.9449	0.97734	0.97741	0.99503	0.99979	0.99932	0.99593
8–18-1	*0.99282*	*0.99791*	*0.98743*	*0.99358*	0.99338	0.99547	0.96979	0.99157
8–19-1	0.98772	0.97465	0.95	0.98377	0.99939	0.99798	0.99937	0.99922
8–20-1	0.94084	0.9568	0.86921	0.93422	0.99246	0.99995	0.97513	0.99492
Networks	Training	Testing	Validation	Overall				
	KwaZulu Natal coalfield							
8–2-1	0.89226	0.73456	0.87592	0.86812				
8–3-1	0.8899	0.88621	0.93619	0.89694				
8–4-1	0.86274	0.91721	0.87234	0.88062				
8–5-1	0.95628	0.97023	0.96165	0.95996				
8–6-1	0.97768	0.87992	0.98121	0.97445				
8–7-1	0.96428	0.97414	0.93981	0.96324				
8–8-1	0.98663	0.96566	0.95338	0.98095				
8–9-1	0.98088	0.96532	0.94928	0.97607				
8–10-1	0.98718	0.97146	0.99117	0.98392				
8–11-1	0.98055	0.99352	0.96196	0.98144				
8–12-1	0.99093	0.97725	0.97161	0.98656				
8–13-1	0.97832	0.96676	0.97698	0.97658				
8–14-1	0.97614	0.99108	0.96822	0.97663				
8–15-1	0.9598	0.95852	0.98119	0.9627				
8–16-1	0.99026	0.99316	0.95623	0.98676				
8–17-1	*0.99732*	*0.99553*	*0.99438*	*0.99673*				
8–18-1	0.9896	0.97838	0.99088	0.9893				
8–19-1	0.98635	0.99745	0.98239	0.98853				
8–20-1	0.99078	0.99682	0.99888	0.99336				

revolutions. The final grind was then screened using a 75 μm sieve, and the under-size (−75 μm) fines formed were weighed and the grindability was determined from Eq. (1).

$$HGI = 13 + 6.93W \tag{1}$$

where W is the weight of the test sample passing through a 75 μm sieve after grinding.

The AI was determined according to a British standard [11] based on the Yancey, Gear and Price (1951) method with some modifications. This was accomplished by mechanically grinding 4 kg of coal in a steel pot, thoroughly levelled out over the blades and covered with a steel lid. Having introduced the coal into the steel pot, the stirrer rotated for 12, 000 revolutions at 1,500 rpm. The abrasiveness index was determined after the test from the loss of mass in milligrammes of the blades from its initial mass and mass after grinding. The statistics of the outcome of the experimental results are presented in Tables 1 to 3.

3. Results and discussions

The statistics of the outcome of the experimental results and their respective correlation coefficient matrix are presented in Tables 1-6. The mean values of calorific value, moisture content, ash content, volatile matter, fixed carbon, total sulphur, pyrite, HGI and AI are 26.92, 3.371, 14.721, 26.329, 55.576, 0.696, 0.820, 54.959, and 122.680 respectively for the Witbank samples. The mean values for the samples from Ermelo coalfield, following the same order as Witbank samples are 25.837, 3.866, 17.020, 23.745, 55.3701, 0.731, 0.757, 57.304 and 131.536 respectively, while for the KwaZulu Natal coalfield are 29.798, 1.819, 13.394, 12.580, 72.196, 1.111, 0.955, 54.281 and 89.831 respectively. There are no large deviations in the parameter values except the AI for the three locations. The distribution of parameters for Witbank coalfield is moderately skewed, except for total sulphur, pyrite, and AI, which are highly skewed. For the Ermelo coalfield, only fixed carbon and AI are highly skewed while other parameters are moderately skewed. The KwaZulu Natal coalfield has volatile matter, pyrite and total sulphur that are highly skewed, while others have a moderately skewed trend. The kurtosis of the parameters are largely platykurtic distributions except for total sulphur, pyrite and AI in the case of Witbank coalfield, AI only in the case of Ermelo coalfield and total sulphur and pyrite in the case of KwaZulu Natal coalfield which are leptokurtic in their distributions.

As coal properties have a significant impact on AI, it is essential to develop reliable models that can account for the non-linearity between the input and output variables. This can be achieved by adopting soft computing techniques and comparing the results for the different coalfields. The outcome of this prediction will reveal which predictive model is more reliable and appropriate to individual South African coalfields. This will be beneficial as it will allow inference of coal properties that have affected the reported AI values.

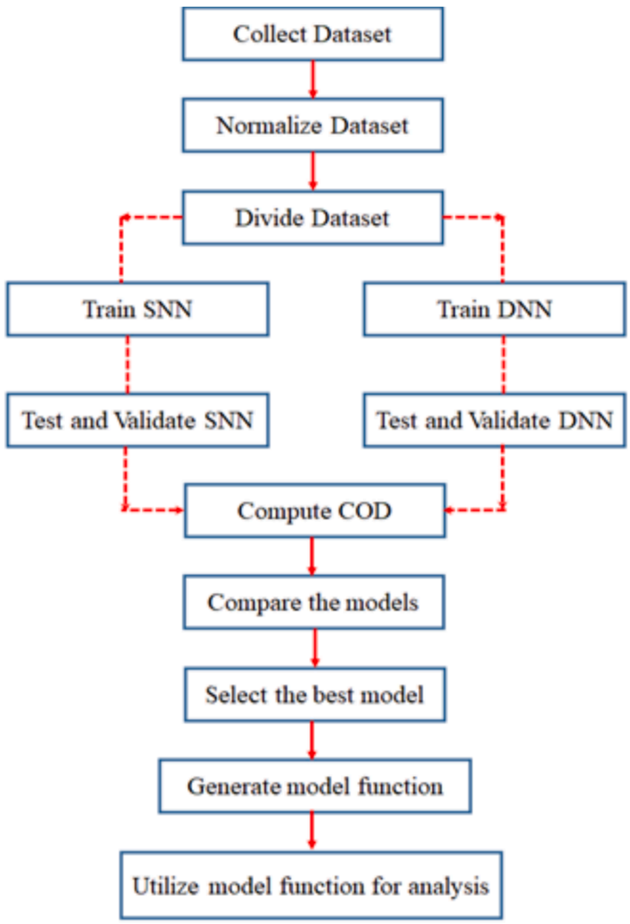

Fig. 2. The adopted procedures for the SNN and DNN.

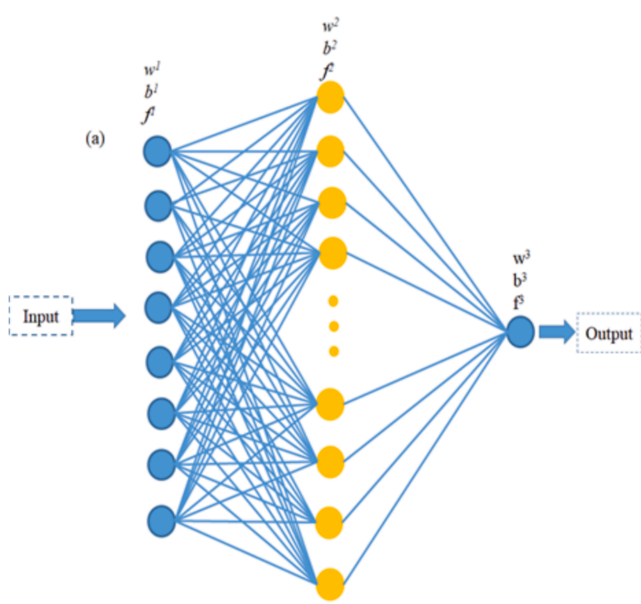

Fig. 3. Typical SNN structure.

3.1. Development of predictive models for abrasive index

3.1.1. SNN model

The SNN was developed in this study for the AI of the coal samples sourced from different coalfields in South Africa. The SNN was implemented in the MATLAB. To achieve this, the pre-processed data was loaded into the MATLAB. Then, the ANN parameters such as the transfer function, number of neurons in the hidden layer and the number of hidden layers were defined including the backpropagation training algorithm coupled with the Levenberg Marquardt optimizer. The tan-sigmoid transfer function was used on both the hidden and output layers. The network was trained by partitioning the data into training, testing, and validation datasets. Furthermore, the network was iteratively trained with varying numbers of neurons in the hidden layer, ranging from 2 to 20, for each of the three coalfields where samples were taken. For the Witbank coalfield, the 8–18-1 network gave the optimum R-values for the training, testing and validation phases, while the 8–12-1 network gave the optimum for the Ermelo coalfield and the 8–17-1 network is the best for the KwaZulu Natal coalfield (Table 7). The adopted procedures and typical SNN structure are shown in Figs. 2 and 3.

3.1.2. DNN model

To enhance the performance of the SNN, the DNN, which is in essence an increase or addition of more hidden layers to the SNN, was used in this study. According to Lim et al. [21], the DNN has hidden layers that are greater than or equal to three. The DNN is adopted in this study to enhance the performance of the SNN. The procedures followed in implementing the DNN are similar to the SNN except that there are more hidden layers. Three hidden layers were employed in this study for the three different locations. The strategy adopted was that the optimum SNN as presented in Table 4 for each of the locations was subject to the DNN. The determination of the number of neurons in each hidden layer was achieved based on a trial and error approach [22]. The transfer functions used for the hidden and output layers are tansigmoid functions. Three hidden layers are used in all the locations. The summary of the procedures adopted is presented in Fig. 2. A typical DNN structure is also shown in Fig. 4. The DNN procedures followed are similar to that of Maleki et al. [22],Maleki et al. [23] as shown in Fig. 2. The 8–17-19–19-1, 8–12-19–19-1 and 8–18-26–26-1 DNN structures are used for the Witbank, Ermelo and KwaZulu Natal coals respectively.

3.2. Comparison of proposed models

The proposed models which are SNN and DNN were correlated as presented in Figs. 5 to 13 for the training, testing and validation cases for each of the three locations. For the samples from Witbank coalfield, there is a strong correlation between the measured and predicted AI for the three phases as the training, testing and validation have R values of 0.9926, 0.9979 and 0.9874 respectively (Figs. 5 to 7) for SNN. This observation holds true for the DNN, but the R-values of the DNN model are stronger for the three phases than the SNN model. For the Ermelo coals, the R-values obtained for the training, testing, and validation phases of the SNN are 0.99997, 0.99999, and 0.99955 (Figs. 8 to 10). These R-values are very strong enough to give reliable prediction of the AI but the DNN model was developed for the other locations. The R values obtained for the three phases using DNN are 1, which is the optimal R-value that can ever be obtained. This implies that the DNN model can give a reliable prediction of the AI. For the KwaZulu Natal coals, the R-values obtained for the training, testing and validation phases are 0.9973, 0.9955 and 0.9944 (Figs. 11 to 13) respectively using the SNN model. The obtained R-values are strong enough to give reliable prediction of the AI but the DNN R-values which are 0.9991, 0.9997 and 0.9999 respectively for the training, testing and validation phases are stronger than those of the SNN. This implies that the DNN is more accurate and reliable than the SNN models for all three cases.

Inspired by Maleki et al. [22],Maleki et al. [23], the relevant model function can be written for the DNN with 5 layers as presented in Eq. (2).

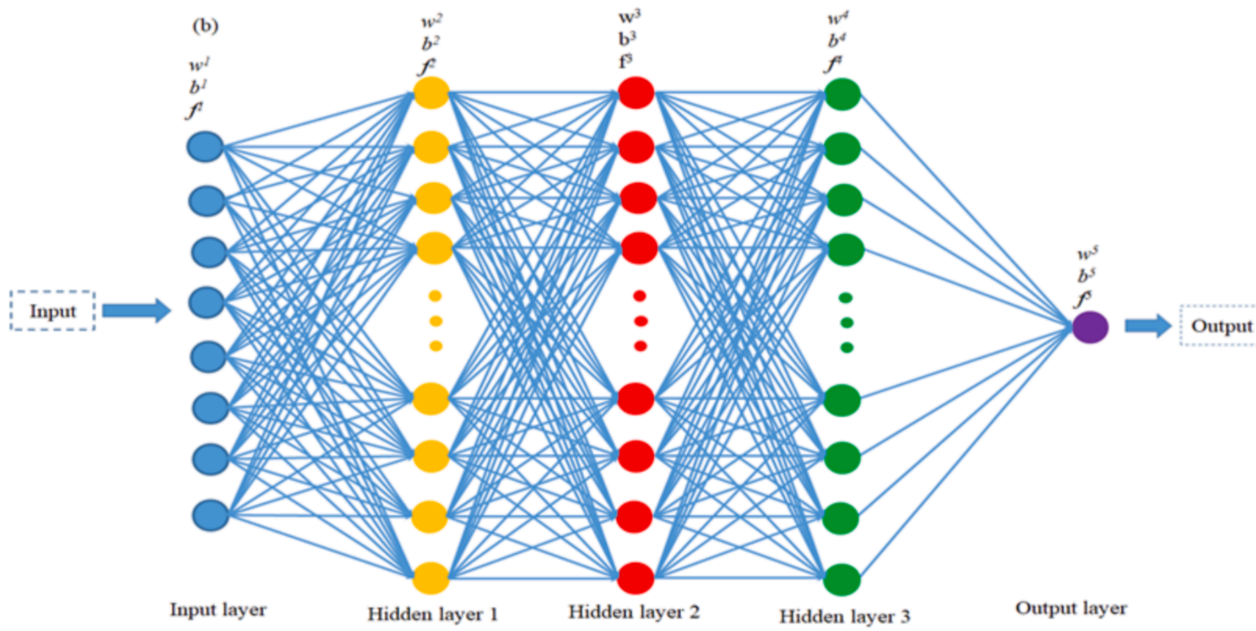

Fig. 4. Typical DNN structure.

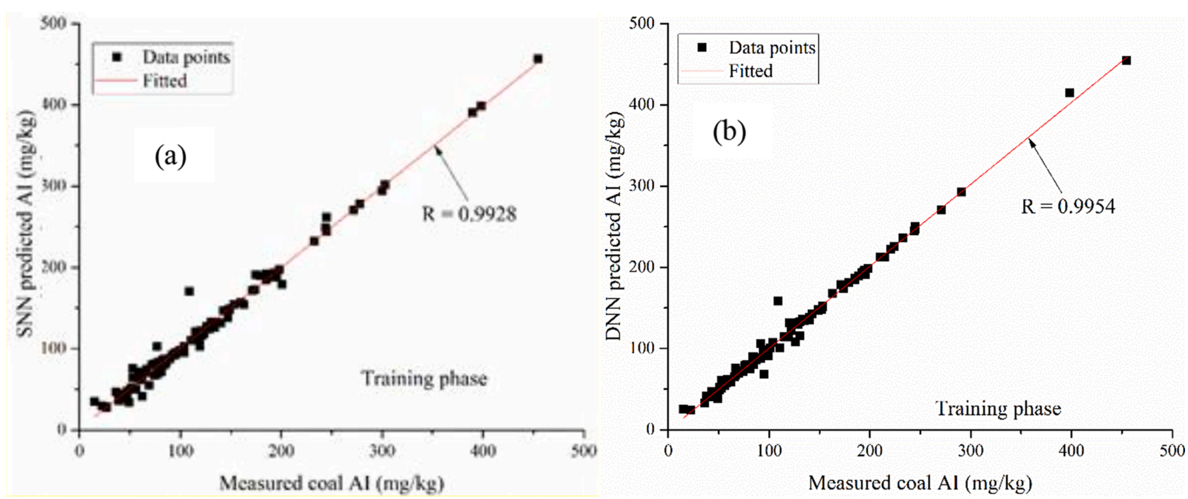

Fig. 5. Correlation of the measured and predicted AI with (a) SNN and (b) DNN models for training phase in Witbank Coals.

$$out(O_1) = L^5 = f^5\left(w^5 f^4\left(w^4 f^3\left(w^3 f^2\left(w^2 f^1\left(w_i^1 + b^1\right) + b^2\right) + b^3\right) + b^4\right) + b^5\right) \quad (2)$$

where f^1 to f^5 are the transfer functions, w^1 to w^5 are the obtained weights and b^1 to b^5 are the obtained biases. With this function, the DNN model outputs can be computed.

3.3. Statistical evaluation of the models

The statistical evaluations of the proposed models are conducted using the coefficient of determination (R^2), root mean square error (RMSE), mean absolute error (MAE) and mean absolute percentage error (MAPE) as presented in Eqs. (3) to (6).

$$R^2 = \left(\frac{\sum_{i=1}^{n} (\Delta_i - \Delta^-)(\chi_i - \chi^-)}{\sqrt{\sum_{i=1}^{n} (\Delta_i - \Delta^-)^2 \sum_{i=1}^{n} (\chi_i - \chi^-)^2}} \right)^2 \quad (3)$$

$$MAE = \frac{\sum_{i=1}^{n} |\Delta_i - \chi_i|}{n} \quad (4)$$

$$RMSE = \sqrt{\frac{\sum_{i=1}^{n} (\Delta_i - \chi_i)^2}{n}} \quad (5)$$

$$MAPE = \frac{\sum_{i=1}^{n} \left| \frac{\Delta_i - \chi_i}{\Delta_i} \right|}{n} \times 100\% \quad (6)$$

where Δ and χ are the measured and predicted values while Δ^- and χ- are their respective mean values. The obtained results using Eqs. (3) to (6)

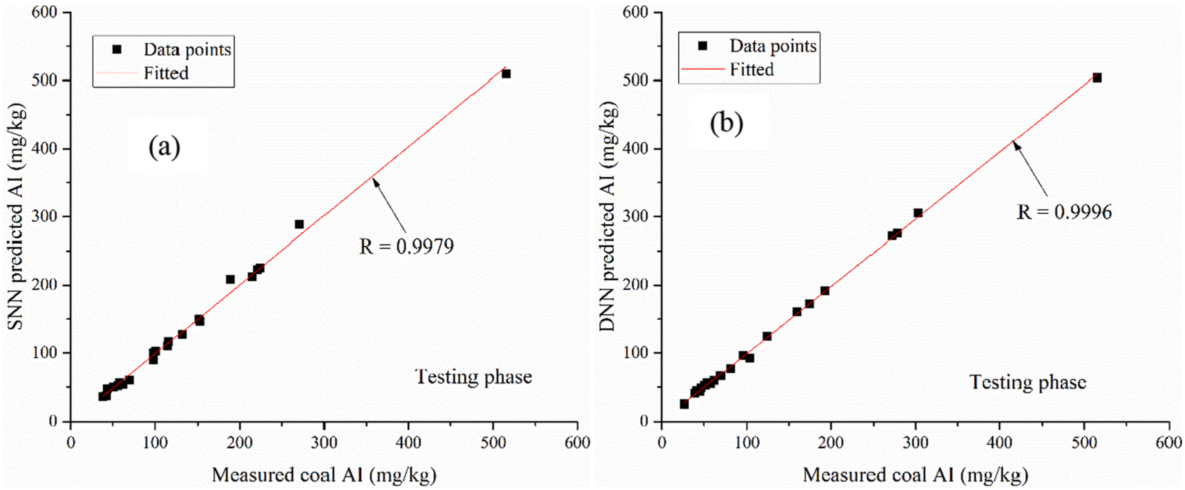

Fig. 6. Correlation of the measured and predicted AI with (a) SNN and (b) DNN models for testing phase in Witbank Coals.

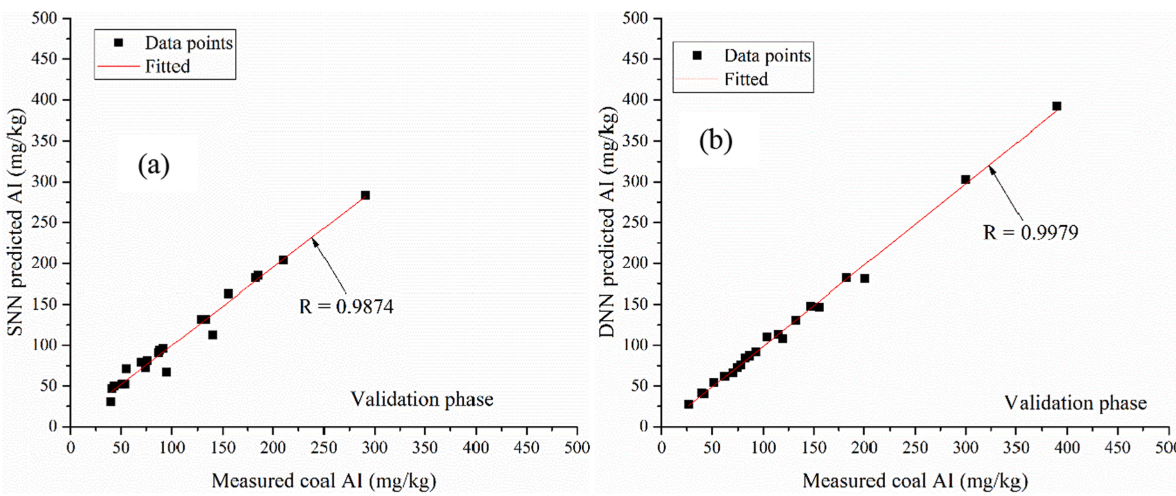

Fig. 7. Correlation of the measured and predicted AI with (a) SNN and (b) DNN models for training phase in Witbank Coals.

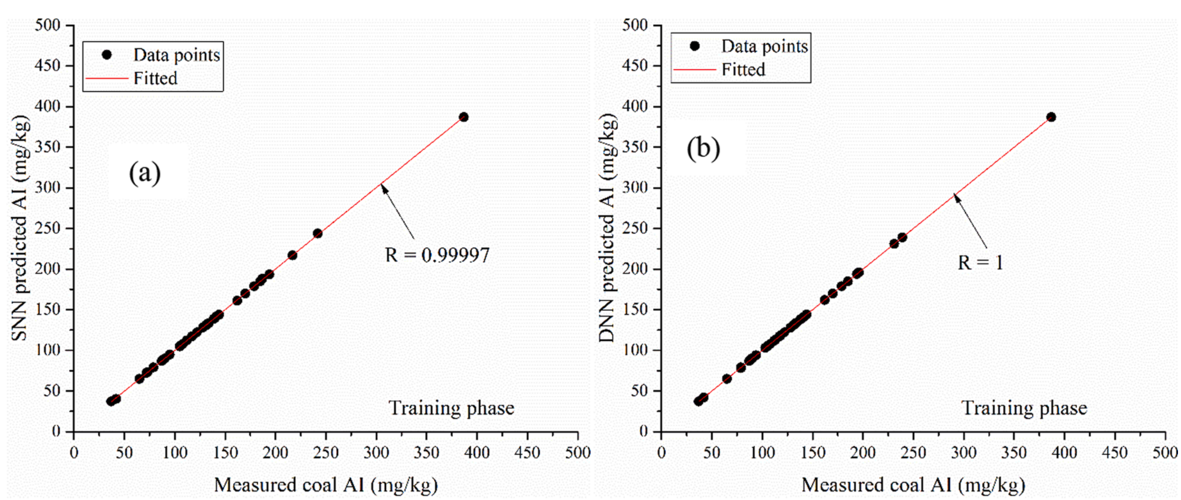

Fig. 8. Correlation of the measured and predicted AI with (a) SNN and (b) DNN for training phase in Ermelo Coals.

for the three locations are presented in Table 8. For the Witbank coals using SNN, R^2, RMSE, MAE and MAPE obtained are 0.9857, 9.73904, 5.8043 and 5.3299 for the training phase, 0.9979, 7.2014, 5.3358 and 8.6357 for the testing phase and 0.975, 10.2191, 6.9454 and 8.0717 for the validation phase. The obtained R^2, RMSE, MAE and MAPE for the training phase using DNN are 0.9908, 7.2329, 2.9646 and 3.054

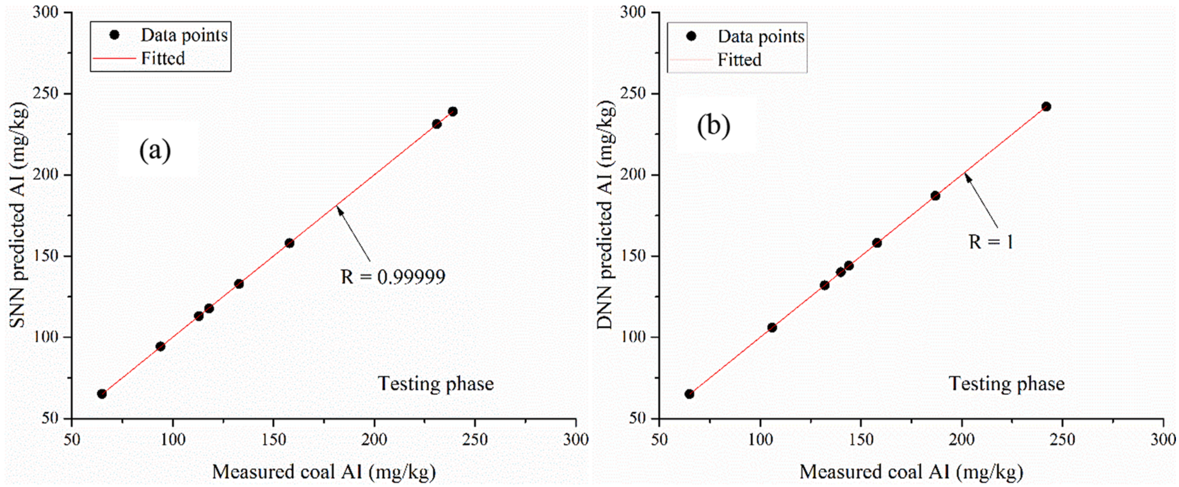

Fig. 9. Correlation of the measured and predicted AI with (a) SNN and (b) DNN for testing phase in Ermelo Coals.

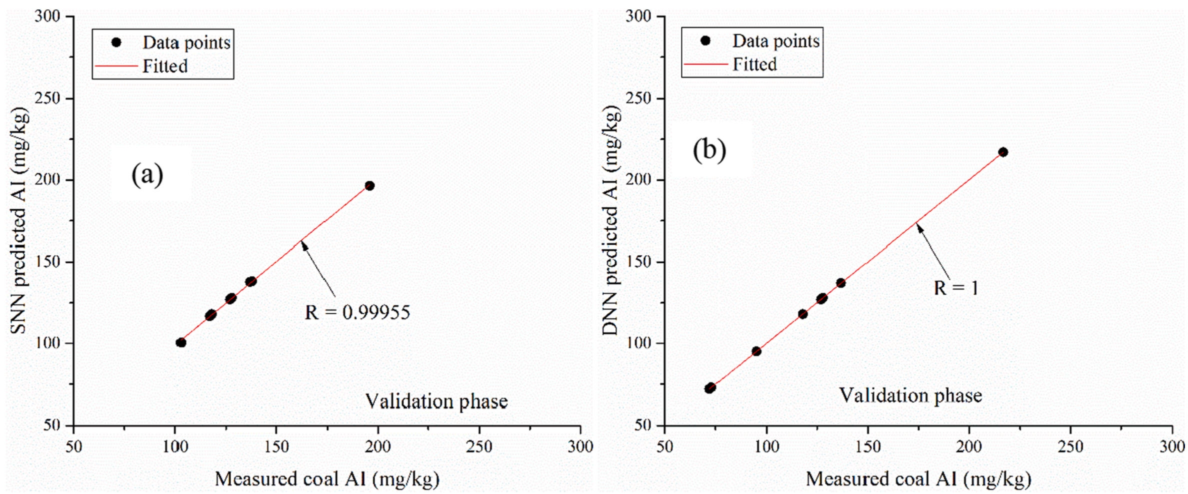

Fig. 10. Correlation of the measured and predicted AI with (a) SNN and (b) DNN for validation phases in Ermelo coals.

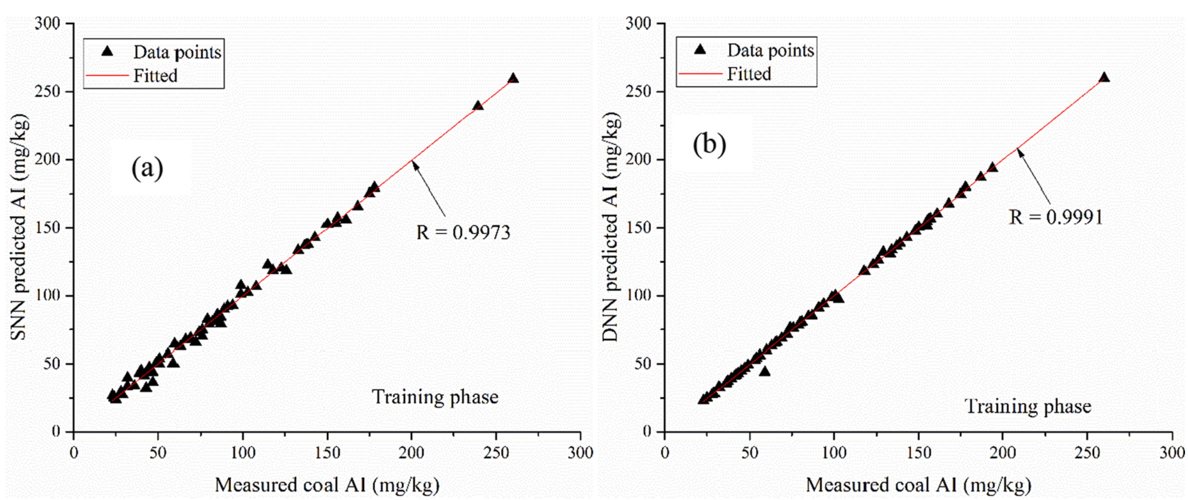

Fig. 11. Correlation of the measured and predicted AI with (a) SNN and (b) DNN for training phase in KwaZulu Natal Coals.

respectively. For the testing phase, they are 0.9992, 3.9742, 2.6177, and 2.9298. For the validation phase, they are 0.9958, 5.7102, 3.4003, and 3.0375 respectively. For Ermelo coals, R^2, RMSE, MAE and MAPE obtained using SNN are 0.9999, 0.485014, 0.2377 and 0.2319 for the training phase, 0.99999, 0.2029, 0.1643 and 0.1518 for the testing phase and 0.9991, 0.9755, 0.5235 and 0.4536 for the validation phase.

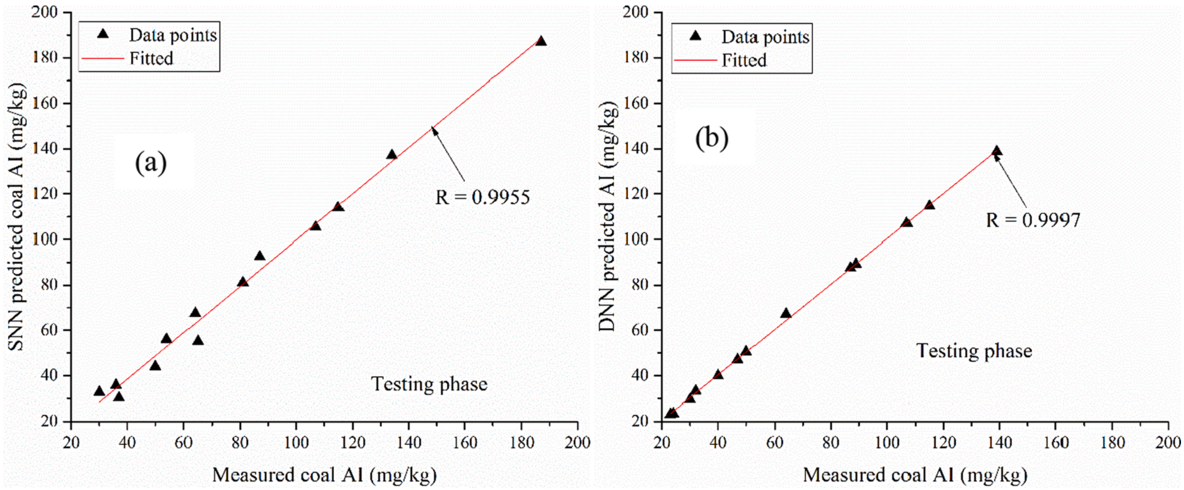

Fig. 12. Correlation of the measured and predicted AI with (a) SNN and (b) DNN for testing phase in KwaZulu Natal Coals.

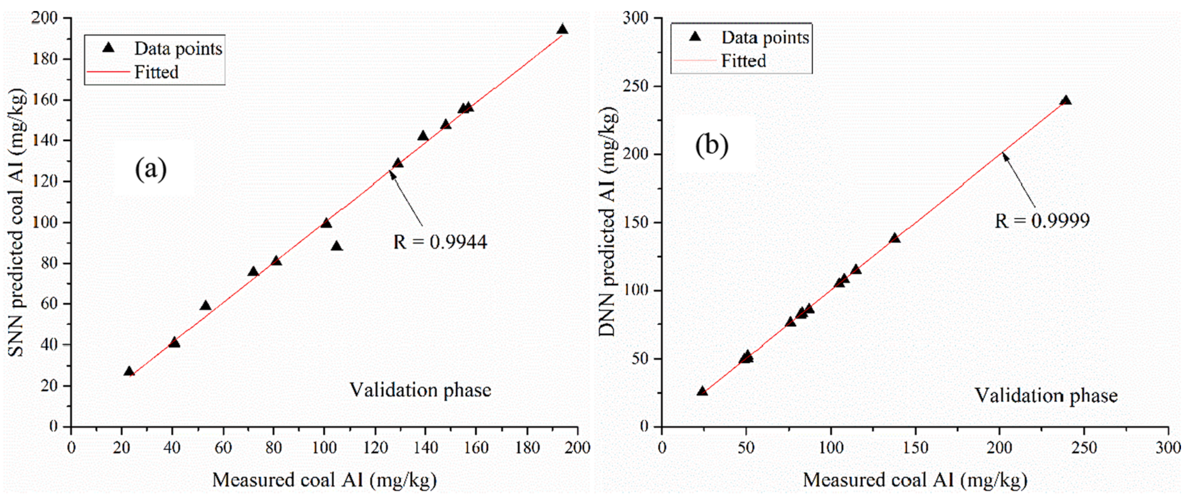

Fig. 13. Correlation of the measured and predicted with (a) SNN and (b) DNN for validation phase in KwaZulu Natal Coals.

Table 8
Statistical evaluations of the models.

	R^2	RMSE	MAE	MAPE	
Witbank coalfield					
SNN	0.9857	9.739043	5.804293	5.329881	Training
DNN	0.99084	7.232865	2.964595	3.053977	
SNN	0.9979	7.20141	5.335846	8.635705	Testing
DNN	0.9992	3.974177	2.617705	2.929832	
SNN	0.975	10.21909	6.945353	8.071698	Validation
DNN	0.9958	5.710179	3.400264	3.037507	
Ermelo coalfield					
SNN	0.9999	0.485014	0.237608	0.231884	Training
DNN	1	0.128091	0.021058	0.027044	
SNN	0.99999	0.202881	0.164256	0.151751	Testing
DNN	1	0.000137	6.52E-05	4.15E-05	
SNN	0.9991	0.975508	0.523499	0.453604	Validation
DNN	1	0.018243	0.006468	0.004728	
KwaZulu Natal coalfield					
SNN	0.9946	3.813836	2.661783	4.579677	Training
DNN	0.9983	2.196114	0.77925	1.046391	
SNN	0.9911	4.369585	3.283544	5.844786	Testing
DNN	0.9994	0.998426	0.59701	1.273221	
SNN	0.9888	5.268629	2.894087	4.19863	Validation
DNN	0.9999	0.681385	0.441831	1.006586	

The obtained R^2, RMSE, MAE and MAPE for the training phase using DNN are 1, 0.1281, 0.0211 and 0.0270 while for the testing phase, they are 1,0.0003,6.52E-05 and 4.15E-05 and for the validation phase, they are 1,0.0182,0.0065 and 0.0047 respectively. For Ermelo Coals, the SNN model has shown very good performance for all three phases, but the DNN has slightly increased the SNN performance. For KwaZulu Natal coals, the obtained values of the statistical indicators in Eqs. (3) to (6) using the SNN models have significantly increased the R^2-values in all three phases using the DNN while RMSE, MAE and MAPE have significantly reduced (Table 5). In all the phases, the DNN model has the highest R^2 values with the lowest RMSE, MAE and MAPE. This implies that the performance of the SNN can be significantly improved using the DNN like some of the nature-inspired or other optimization algorithms which have been previously used in different studies for improving the performances of the SNN.

The obtained statistical results presented in Table 8 and explained above are further substantiated by the ANOVA analysis presented in Table 9. The p-value obtained for the three phases for all three coalfields is below the alpha value of 0.05 which implies that the null hypothesis can be rejected and then the F-value can be used to explain the model. The F-values obtained for the DNN models are all greater than those of SNN models which implies that the higher the F-values, the better the statistical indicator R^2 and the lower the statistical indicators RMSE, MAE and MAPE (Table 8). For example, for the Ermelo coals where the

Table 9
ANOVA of the model results.

	DF	Sum of Squares	Mean Square	F Value	Prob > F	Sum of Squares	Mean Square	F Value	Prob > F
		SNN				DNN			
	Training (Witbank coalfield)								
Model	1	668926.9	668926.9	6956.736	0	575873.6	575873.6	10920.43	0
Error	101	9711.683	96.15527			5326.094	52.73361		
Total	102	678638.6				581199.6			
	Testing								
Model	1	255405.7	255405.7	4776.326	0	296818.9	296818.9	23634.19	0
Error	20	1069.465	53.47326			251.1775	12.55888		
Total	21	256475.2				297070.1			
	Validation								
Model	1	82209.63	82209.63	780.7913	0	156547.1	156547.1	4772.242	0
Error	20	2105.803	105.2901			656.0737	32.80369		
Total	21	84315.43				157203.2			
	Training (Ermelo coalfield)								
Model	1	148617.9	148617.9	640920.4	0	145205.4	145205.4	8.75E + 06	0
Error	38	8.81152	0.23188			0.63082	0.0166		
Total	39	148626.7				145206			
	Testing								
Model	1	27268.13	27268.13	506961.8	5.55E-16	19433.5	19433.5	9.10E + 11	0
Error	6	0.32272	0.05379			1.28E-07	2.14E-08		
Total	7	27268.45				19433.5			
	Validation								
Model	1	5674.83	5674.83	6689.517	2.25E-10	14948.53	14948.53	3.93E + 07	0
Error	6	5.0899	0.84832			0.00228	3.81E-04		
Total	7	5679.92				14948.53			
	Training (KwaZulu Natal coalfield)								
Model	1	168654	168654	11318.96	0	170378.5	170378.5	35581.64	0
Error	61	908.908	14.90013			292.0913	4.78838		
Total	62	169562.9				170670.6			
	Testing								
Model	1	25731.67	25731.67	1221.611	1.26E-12	17672.22	17672.22	16889.41	0
Error	11	231.701	21.06373			11.50984	1.04635		
Total	12	25963.38				17683.73			
	Validation								
Model	1	30563.38	30563.38	969.6302	4.44E-12	34667.7	34667.7	72986.26	0
Error	11	346.7272	31.52065			5.22488	0.47499		
Total	12	30910.11				34672.93			

prediction performance of SNN is very high, there is a clear difference in the F-values obtained for the DNN and SNN models for three phases with the former having the highest value and consequently, the optimum model performance (Table 8).

3.4. Sensitivity analysis

The sensitivity analysis/relative contribution of each of the model inputs on the predicted outputs is investigated using the cosine amplitude method of Yang and Zhang [40] as presented in Eq. (7). This method is selected because it has been widely used among the researchers and it has shown a strong ability in predicting the relative contribution of the model input variables to the predicted output [20].

$$\mathrm{RI} = \frac{\sum_{i=1}^{m}(MI_i \times MO_i)}{\sqrt{\sum_{i=1}^{m}(\mathrm{MI}_i)^2 \times \sum_{i=1}^{m}(MO_i)^2}} \tag{7}$$

where MI is the model input variable and MO is the model predicted output. The outcomes of the sensitivity analysis of the trained datasets for the Witbank, Ermelo and KwaZulu Natal coalfields as presented in Fig. 14 revealed that the ash content is the most influencing parameter in all the three coalfields.

4. Conclusions

The abrasive constituents in coal can severely shorten the service life of coal handling equipment, especially the coal grinding mill. The abrasiveness of coal varies depending on its chemical, physical, mechanical, and other characteristics. The AI of coals can be influenced by some of these properties. The study examines eight coal characteristics from 292 coal samples from three South African coalfields that influence their AI, and the following are revealed.

a) The AI is influenced by the various characteristics of coal, which are distinct for coals from different deposits tested.
b) The moisture, volatile matter, ash content, fixed carbon, total sulphur, pyrite, and HGI were found to be non-statistically correlated with the AI values in most cases for individual coalfields of the investigated population of coals.
c) The DNN model is the most reliable and appropriate for all three coalfields with the coefficient of correlation of 0.9992 and 0.9958 for the testing and validation phases in Witbank coalfield. For the Ermelo coalfield, the coefficient of determination 1 is obtained for the testing and validation phases, while that of the KwaZulu Natal coalfield are 0.9994 and 0.9999 for the testing and validation phases, respectively.
d) The sensitivity analysis conducted revealed that the predicted AI in all three coalfields is most influenced by the ash content.

CRediT authorship contribution statement

Moshood Onifade: Writing – review & editing, Writing – original draft, Validation, Supervision, Software, Project administration, Methodology, Investigation, Formal analysis, Data curation, Conceptualization. **Abiodun Ismail Lawal:** Writing – review & editing, Writing – original draft, Validation, Software, Methodology, Investigation, Formal analysis. **Samson Oluwaseyi Bada:** Writing – review & editing, Writing – original draft, Validation, Software, Methodology, Investigation, Resources, Funding acquisition, Data curation, Formal analysis,

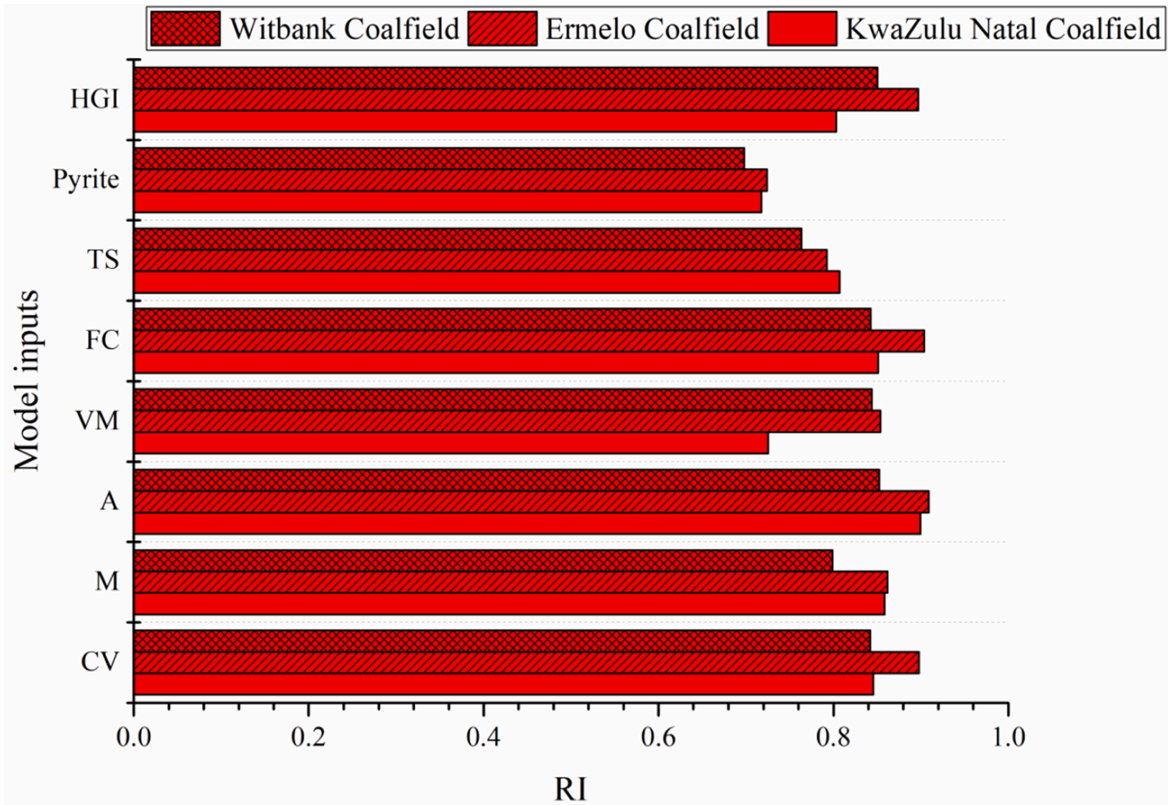

Fig. 14. Relative impacts of the input parameters on the output.

Conceptualization. **Manoj Khandelwal:** Writing – review & editing, Writing – original draft, Validation.

Declaration of competing interest

The authors declare that they have no known competing financial interests or personal relationships that could have appeared to influence the work reported in this paper.

Data availability

Data will be made available on request.

References

[1] Alekhnovich AN, Artemieva NV, Bogomolov VV. Definition and assessment of coal abrasivity. Power Technol Eng 2021;55(1):16–23.
[2] Alkayem NF, Shen L, Mayya A, Asteris PG, Fu R, Luzio GD, Strauss A, Cao M. Prediction of concrete and FRC properties at high temperature using machine and deep learning: a review of recent advances and future perspectives. J Building Eng 2024;83:108369.
[3] Ananda-Babu K, Lawrence A, Sivashanmugam P. Grindability studies on blended coals of high-ash Indian coals with low-ash imported coals. Int J Coal Prep Util 2018;38:433–42.
[4] ASTM. Standard Practice for Preparing Coal Samples for Analysis. 2021.
[5] ASTM. Standard Test Methods for Proximate Analysis of the Analysis Sample of Coal and Coke by Instrumental Procedures. 2010.
[6] ASTM. Standard Test Methods for Determination of Carbon, Hydrogen, and Nitrogen in Analysis Samples of Coal and Carbon in Analysis Samples of Coal and Coke. 2015.
[7] ASTM. Standard Test Method for Gross Calorific Value of Coal and Coke. 2017.
[8] ASTM. Standard Test Method for Tumbler Test for Coke. 2021.
[9] Asteris, P. G., Tsaris, A. K., Cavaleri, L., Repapis, C. C., Papalou, A., Trapani, F. D., Karypidis, D. F., (2016). Prediction of the Fundamental Period of Infilled RC Frame Structures Using Artificial Neural Networks. Computational Intelligence and Neuroscience. doi.org/10.1155/2016/5104907.
[10] Bandopadhyay AK. A study on the abundance of quartz in thermal coals of India and its relation to abrasion index: development of predictive model for abrasion. Int J Coal Geol 2010;84(1):63–9.
[11] Standard B. Methods for analysis and testing of coal and coke part 19: Determination of the index of abrasion of coal. BSI- BS 1016–19 British standard institution. United Kingdom; 1980.
[12] Deniz V, Umucu Y. Interrelationships between the bond grindability with physicomechanical and chemical properties of coals. Energy Sources Part A 2013; 35:144–51.
[13] Emad W, Mohammed AS, Bras A, Asteris PG, Kurda R, Muhammed Z, et al. Metamodel techniques to estimate the compressive strength of UHPFRC using various mix proportions and a high range of curing temperatures. Constr Build Mater 2022;349:128737.
[14] Grzegorzek W, Adamecki D, Głuszek G, Lutynski A, Kowol D. Technique to investigate pulverizing and abrasive performance of coals in mineral processing systems. Energies 2021;14:7300.
[15] Idris A, Man Z, Bustam A, Rabat NE, Uddin F, Mannan HA. Grindability and abrasive behaviour of coal blends: analysis and prediction. Int J Coal Prep Util 2022;42(4):1143–69.
[16] ISO 19579: 2006. Solid mineral fuels Determination of sulphur by IR spectrometry.
[17] Kabuba, J., 2016. Application of Neural Networks Technique for Predicting of Abrasiveness Characteristics of Thermal Coal. Proceedings of the World Congress on Engineering and Computer Science 2016 Vol II WCECS 2016, October 19-21, 2016, San Francisco, USA.
[18] Khandelwal M, Singh TN. Prediction of macerals contents of Indian coals from proximate and ultimate analyses using artificial neural networks. Fuel 2010;89(5): 1101–9.
[19] Khandelwal M, Mahdiyar A, Armaghani DJ, Singh TN, Fahimifar A, Faradonbeh RS. An expert system based on hybrid ICA-ANN technique to estimate macerals contents of Indian coals. Environ Earth Sci 2017;76:399. https://doi.org/10.1007/s12665-017-6726-2.
[20] Lawal AI, Kwon S. Development of mathematically motivated hybrid soft computing models for improved predictions of ultimate bearing capacity of shallow foundations. J Rock Mech Geotech Eng 2023;15(3):747–59.
[21] Lim J, Jeong S, Lim S, Cho H, Shim JY, Hong SI, Kwon SC, Lee H, Moon I, Kim J. Development of dye exhaustion behaviour prediction model using deep neural network. Proce 14th Int Symposium on Process Systems Eng, Elsevier 2022: 1825–30.
[22] Maleki E, Unal O, Seyedi Sahebari SM, Reza Kashyzadeh K, Danilov I. Application of deep neural network to predict the high-cycle fatigue life of AISI 1045 steel coated by industrial coatings. J Marine Sci Eng 2022. https://doi.org/10.3390/jmse10020128.
[23] Maleki E, Unal O, Guagliano M, Bagherifard S. Analysing the fatigue behaviour and residual stress relaxation of gradient nano-structured 316L steel subjected to the shot peening via deep learning approach. Met Mater Int 2022;28:112–31.
[24] Nahvi SM, Shipway PH, McCartney DG. Effects of particle crushing in abrasion testing of steels with ash from biomass-fired power plants. Wear 2009;267:34–42.

[25] Nguyen N-H, Vo TP, Lee S, Asteris PG. Heuristic algorithm-based semi-empirical formulas for estimating the compressive strength of the normal and high-performance concrete. Constr Build Mater 2021;304:124467.
[26] Raask E. Minerals Impurities in coal Combustion: Behaviour. Problems and Remedial measures: Hemisphere Publishing Corporation; 1985. p. 41.
[27] RF State Standard GOST 30827–2002. Solid Mineral Fuel. Definition of Abrasive Capacity (Abrasivity) [in Russian], effective date: January 01, 2004, IPK Izd. Standartov, Moscow (2003).
[28] Sciezska SF. New concepts for determination of pulverised properties of coal. Fuel 1985;64:1132–41.
[29] Singh H, Kumar S, Mishra R, Mohapatra SK, Singh A, Kumar S. Flow characteristics of microwave treated Indian coal: a deep learning modelling. Adv Powder Technol 2023;34(10):104202.
[30] Snyman, C. P., 1998. Coal in Wilson. M. G. C and Anhausser. C. R (Eds). The Mineral deposits of South Africa, Handbook. Council of Geoscience, pp. 136-205.
[31] Spero C. Assessment and prediction of coal abrasiveness. Fuel 1990;69(9):1168–76.
[32] Spero C, Hargreaves DJ, Kirkcaldie RK, Flitt HJ. Review of test methods for abrasive wear in ore grinding. Wear 1991;146:389–408.
[33] Taole RL, Falcon RMS, Bada SO. The impact of coal quality on the efficiency of a spreader stoker boiler. Southern African Institute of Mining And Metallurgy 2015;115:1159–66.
[34] Tshiongo, N., Mulaba-Bafubiandi, A. F., 2013. South African coal and its abrasiveness index determination: An account of challenges, in: Proc. of Southern African Universities Engineering Conf. (SAUPEC), North-West University, otchefstroom, South Africa (2013), pp. 288-293.
[35] Ward CR. Analysis and significance of mineral matter in coal. Int J Coal Geol 2002;50:135–68.
[36] Wells JJ, Wigley F, Foster DJ, Livingston WR, Gibb WH, Williamson J. The nature of mineral matter in a coal and the effects on erosive and abrasive behaviour. Fuel Process Technol 2005;86:535–50.
[37] Wells JJ, Wigley F, Foster DJ, Gibb WH, Williamson J. The relationship between excluded mineral matter and abrasion index of a coal. Fuel 2004;83(3):359–64.
[38] Xie W, He Y, Luo C, Zhang X, Li H, Wang H, et al. Energy-size reduction of coals in the Hardgrove machine. Int J Coal Prep Util 2015;35:51–62.
[39] Xie W, He Y, Qu L, Sun X, Zhu X. Effect of particle properties on the energy-size reduction of coal in the ball-and-race mill. Powder Technol 2018;333:404–49.
[40] Yang Y, Zhang Q. A hierarchical analysis for rock engineering using artificial neural networks. Rock Mech Rock Eng 1997;30:207–22.
[41] Yancey HF, Geer MR, Price JD. An investigation of the abrasiveness of coal and its associated impurities. J Min Eng 1951:262–8.